

EFFECT OF DOPANT CONCENTRATION ON STRUCTURAL PROPERTIES OF CHEMICAL BATH DEPOSITED Mn-DOPED PbS NANOCRYSTALLINE THIN FILMS

L. R. SINGH^{a*}, R. K. L. SINGH^b

^a*Department of Physics, D. M. College of Science, Dhanamanjuri University, Imphal-795001, Manipur (India)*

^b*Department of Chemistry, D. M. College of Science, Dhanamanjuri University, Imphal-795001, Manipur (India)*

Mn-doped PbS nanocrystalline thin films of three different dopant concentrations of 1 wt.%, 1.5 wt.% and 2 wt.% Mn were deposited onto glass substrates at 313K by Chemical Bath Deposition Method (CBD) using lead acetate and thiourea as precursors with Manganese acetate as dopant precursor. The as prepared thin films were characterized by using X-ray diffraction (XRD), Scanning Electron Microscope (SEM), Transmission Electron Microscope (TEM) and Energy Dispersive X-ray (EDAX). Analysis of energy dispersive X-ray confirmed the presence of Pb, Mn and S elements. The particle size of the prepared nanoparticles decrease with the increase of dopant concentrations. For 0 wt.%, 1 wt.%, 1.5 wt.% and 2 wt.% Mn dopant concentrations, the average crystallite sizes were found to be 21 nm, 17 nm, 14 nm and 11 nm respectively. The decrease in crystallite size with the increase in dopant concentrations may be due to the replacement of larger radius lead ions by the smaller radius Mn ions.

(Received October 4, 2019; Accepted July 17, 2020)

Keywords: Nanocrystalline, Thin film, CBD, Dopant, XRD, SEM, TEM

1. Introduction

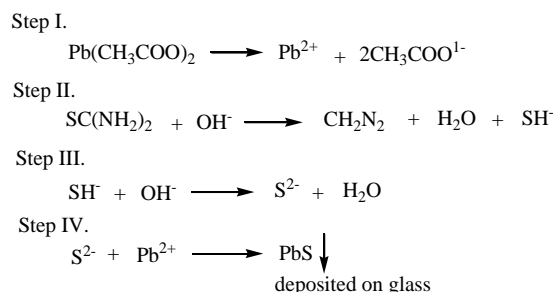
Semiconductor nanomaterials have been the subject of much interest in basic research due to their unique electrical and optical properties different from the materials in bulk form [1-2]. Lead sulphide is an important member of Group IV-VI semiconductors. It has small direct band gap of 0.41 eV at 300 K and a relatively large exciton Bohr radius of 18 nm [3-5]. Below the excitonic Bohr radius, PbS shows strong quantum size effects and the energy band gap of the nanocrystals can be tuned between 0.41 eV and 5.2 eV [6]. It has wide potential applications in various devices like infrared photodetectors, optical switches, sensors, and solar cells [7-9]. For these reasons, many researcher study this material by various deposition techniques such as spray pyrolysis [10], electro deposition [11,12], microwave heating [13,14], successive ionic layer adsorption and reaction (SILAR) [15], vacuum evaporation [16], molecular beam epitaxy [17], chemical deposition [18-21] etc. Among these methods, chemical bath deposition (CBD) has several advantages compared to other techniques such as uniform film deposition, inexpensive, convenient for large area deposition and do not require sophisticated instruments [22,23]. The structural, optical and electrical properties of pure nanocrystalline PbS thin films have been widely reported in the literature. However, number of available literatures in the field of study of Mn-doped PbS nanocrystalline thin films prepared by CBD technique are few. This paper reports the investigation of effect of dopant concentrations on structural properties of Mn-doped nanocrystalline PbS thin films prepared by chemical bath deposition technique.

* Corresponding author: l_rajen03@yahoo.com

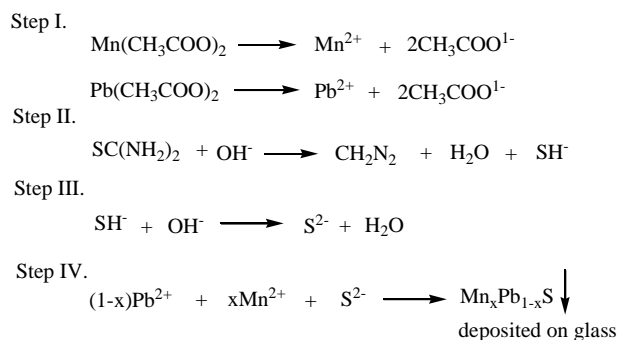
2. Experimental procedure

For the preparation of undoped PbS thin film, pH of 0.2 M lead acetate solution was adjusted to 11 by drop wise addition of NH_3 solution in a beaker. To this solution, equimolar solution of thiourea was added and stirred well by using a magnetic stirrer. Cleaned glass substrates were vertically immersed into the solution and heated at 313 K for 1 hour. The solution was kept overnight at room temperature for complete deposition of nanocrystalline PbS thin film. After deposition, the PbS coated substrates were taken out from the bath and washed repeatedly with deionized water and dried in air at room temperature. The deposited films on the glass substrates were used for XRD, SEM and TEM studies. For preparation of Mn-doped PbS thin films, three sets of 0.2 M lead acetate solutions (premixed with 1 wt.%, 1.5 wt.% and 2 wt.% manganese acetate) were used. The Scheme 1 and Scheme 2 are the reaction mechanisms for the preparation of undoped and Mn-doped PbS thin films respectively. In Scheme 2, $x = 0.01, 0.015$ and 0.02 for dopant percent of 1 wt.%, 1.5 wt.% and 2 wt.% Mn

Scheme 1. The reaction mechanism of preparation of undoped PbS thin film.



Scheme 2. The reaction mechanism of preparation of Mn-doped PbS thin film.



The structure of the films was analyzed by using PANalytical X'Pert Pro X-ray diffractometer (XRD) using CuK_α radiation ($\lambda = 1.5418 \text{ \AA}$). Surface morphology of the films was studied using JEOL-JSM 6360 scanning electron microscope (SEM), particle sizes were determined by using JEM-2100 transmission electron microscope (TEM).

3. Results and discussion

3.1. Phase analysis

Fig. 1 shows the XRD pattern of PbS thin films with Mn dopant concentrations of 0 wt.%, 1 wt.%, 1.5 wt.% and 2 wt.%. The Mn doped PbS thin films show four characteristic peaks at 25.825° , 29.975° , 42.975° and 50.875° which correspond to (111), (200), (220) and (311) planes respectively with preferred growth orientation along (200) plane. The observed peak positions are consistent with the face centered cubic (fcc) crystal structure of PbS (JCPDS No. 5-5921)[24].

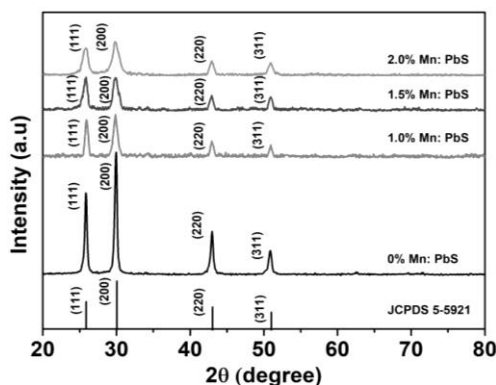


Fig. 1. XRD spectra of PbS thin films at various doping concentrations ($Mn^{2+} = 0$ wt.%, 1 wt.%, 1.5 wt.% and 2 wt.%) along with JCPDS 5-5921.

Table 1 shows the experimentally obtained X-ray diffraction angle (2θ) and standard diffraction angle (2θ) of undoped PbS thin film. Peak indexing is done for undoped PbS using $\sin^2\theta$ method and shown in Table 2. Since, (hkl) values obtained are either all odd or all even, so, the prepared PbS thin film have fcc lattice structure. The XRD parameters of undoped and Mn-doped PbS thin films are shown in Table 3.

Table 1. Standard and experimental diffraction angles of PbS undoped thin film.

Experimental diffraction angle (2θ in degrees)	Standard diffraction angle JCPDS No. 5-5921 (2θ in degrees)
25.825	25.963
29.975	30.074
42.975	43.058
50.875	50.976

Table 2. Indexing of experimental peaks of undoped PbS thin films.

2θ (degree)	θ (radian)	$\sin^2\theta$	$\sin^2\theta_{\min}$	$(3 \times \sin^2\theta / \sin^2\theta_{\min})$	$h^2 + k^2 + l^2$	h k l
25.825	0.225	0.050	0.050	3.000	3	111
29.975	0.262	0.067	0.050	4.018	4	200
42.975	0.375	0.134	0.050	8.061	8	220
50.875	0.444	0.184	0.050	11.084	11	311

Table 3. Structural parameters of undoped and Mn-doped PbS thin films obtained from XRD spectra.

Mn doping level (wt.%)	hkl	2 θ (degree)	FWHM (radian)	Crystallite size, D (nm)	Average crystallite size, D (nm)	d (\AA)	a (\AA)	Average, a (\AA)
0	111	25.825	0.0064	23.076	21	3.450	5.975	5.961
	200	29.975	0.0067	22.507		2.981	5.962	
	220	42.975	0.0075	20.710		2.105	5.953	
	311	50.875	0.0085	18.843		1.795	5.953	
1	111	25.925	0.0084	17.772	17	3.437	5.953	5.960
	200	29.875	0.0119	12.593		2.991	5.981	
	220	42.925	0.0089	17.489		2.107	5.959	
	311	50.925	0.0087	18.449		1.793	5.947	
1.5	111	25.875	0.0119	12.494	14	3.443	5.964	5.963
	200	29.875	0.0148	10.101		2.991	5.981	
	220	42.925	0.0104	14.973		2.107	5.959	
	311	50.925	0.0098	16.415		1.793	5.947	
2	111	25.766	0.0142	10.495	11	3.458	5.989	5.969
	200	29.831	0.0173	8.679		2.995	5.990	
	220	42.985	0.0117	13.320		2.104	5.951	
	311	50.952	0.0122	13.205		1.792	5.944	

The presence of more than one peak indicates that the prepared films are polycrystalline in nature. The narrow peaks show that the material has good crystallinity. The absence of any other additional peaks for the doped film when compare with undoped one suggests the incorporation of Mn^{2+} ions into the Pb lattices and free of impurities. Decreasing of peak intensities and broadening of peaks are observed when dopant concentration is increased. The decrease in peak intensity is due to doping-induced structural disorder [25]. The broadening of peaks may be due to the replacement of larger radius Pb^{2+} (119 pm) ions by smaller radius Mn^{2+} (80 pm) ions. When Mn^{2+} occupies more and more lattice sites originally occupied by Pb^{2+} in host lattice, internal strain increases and crystal structure become unstable. In order to stabilize the crystal, there would be spontaneous size reduction of the particles. As the Mn concentration increases, the diffraction peaks become broader due to reduction in the particle size [26]. The average crystallite size (D) of the films is calculated from the prominent four XRD peaks using the Scherrer's relation [27]

$$D = k\lambda/\beta C \cos\theta \quad (1)$$

where Scherrer constant, $k = 0.94$ (for spherical crystallites with cubic symmetry), β = full width at half maximum (FWHM) of the most intense peak in radian, θ is Bragg's diffraction angle, λ is wavelength of X-ray used (1.5418 \AA). For 0 wt.%, 1 wt.%, 1.5 wt. and 2 wt.%, Mn doped PbS thin films, the average crystallite sizes are 21 nm, 17 nm, 14 nm and 11 nm, respectively (Table 3). The decrease in crystallite size with the increase of dopant concentration may be due to the replacement of larger radius lead ions by smaller radius Mn ions. Similar results are reported for Mn-doped CdS films [28,29]. Variation of crystallite size with dopant concentration is shown in Fig. 2.

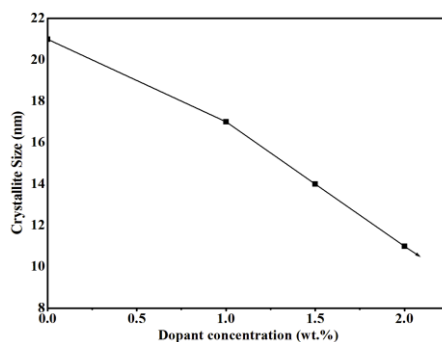


Fig. 2. Dependence of crystallite size on dopant concentration.

3.2. Elemental analysis

The quantitative and qualitative compositional analysis of the as-deposited Mn-doped PbS films is carried out by EDAX technique. Fig. (3-6) show EDAX spectra of 0 wt.%, 1 wt.%, 1.5 wt.% and 2 wt.% Mn-doped PbS thin films respectively. The spectrum of undoped thin film confirms the average atomic percentage of Pb and S as 52.62 and 47.38 respectively showing that the film is Pb rich whereas, other spectra indicate that Mn atoms are incorporated with the PbS film.

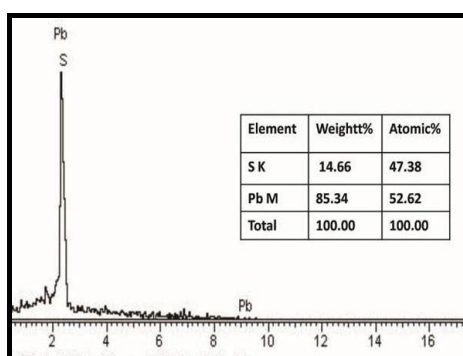


Fig. 3. EDAX spectra of PbS thin film with Mn = 0 wt.%.

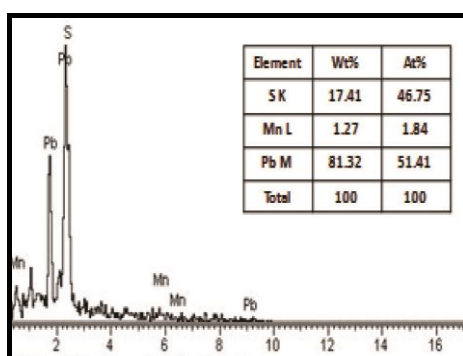


Fig. 4. EDAX spectra of 1 wt.% Mn doped PbS thin film.

It is also observed that atomic percentage of Mn atom increases with increase in dopant concentration. The extra peaks observed in the EDAX spectra correspond to some impurity elements like Mg, Si, Na, Ca which are due to glass substrate or the substrate holder used in the EDAX instrument [30-32]. These might also be due to presence of C and O due to exposure of the film to the atmosphere [33]. There is no source of these elements in the chemicals used for the Mn doped and undoped PbS films synthesis.

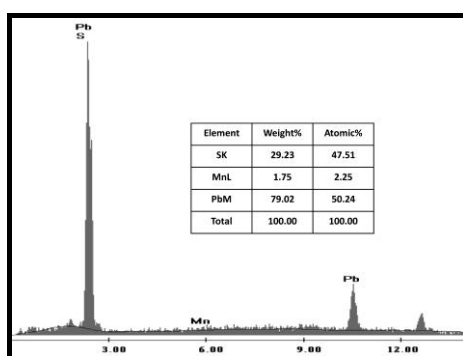


Fig. 5. EDAX spectra of 1.5 wt.% Mn doped PbS thin film.

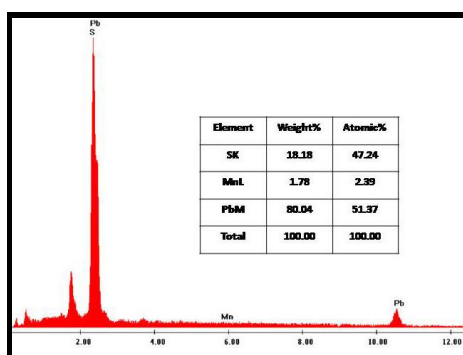


Fig. 6. EDAX spectra of 2 wt.% Mn doped PbS thin film.

3.3. SEM and TEM analysis

Fig.7(a-d) show SEM images of the undoped PbS thin film and another three Mn-doped PbS thin films of different dopant percents. It is observed that the film is continuous over the glass surface and is fairly uniform. The grains of the films have different shapes and sizes but almost compact. There are no macroscopic defects such as voids, peeling or cracks. It is observed that the grains are nearly spherical in shape. All the films are continuous, compact, homogenous and free from voids, cracks or holes.

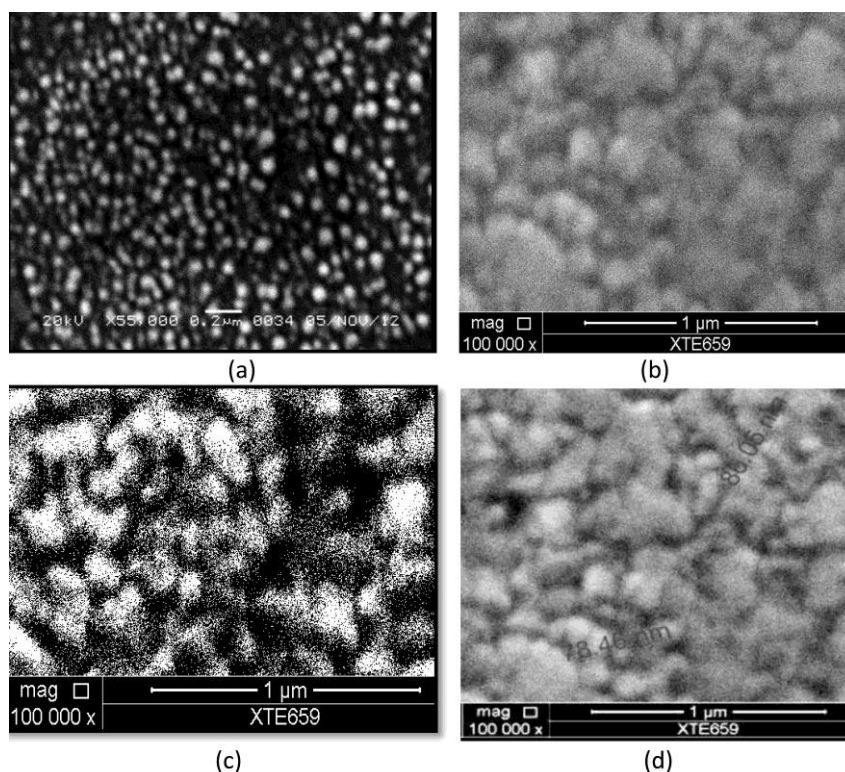


Fig. 7. SEM images of (a) undoped PbS thin film, (b) 1 wt.%, (c) 1.5 wt. % and (d) 2 wt.% Mn-doped PbS thin films.

Fig. 8(a-c) show TEM image, HRTEM image and interplanar spacing ‘d’ and SAED image of undoped PbS thin films. It reveals that small grains are attached together and produce larger grains. The average calculated grain sizes of PbS nanocrystals shown in Fig.8 (a) are found to be in the range 32-46 nm which are greater than the average X-ray diffraction result 21 nm. This difference may be due to the difference in the thickness of the samples, since the TEM grid requires very thin layer deposition on the carbon coated grid, but for XRD characterization thicker film is deposited on the glass substrate [34]. The HRTEM image shown in Fig.8(b) depicts lattice fringe with d-spacing of 0.30 nm corresponding to (200) plane which is in good agreement with the lattice constant for the PbS cubic structure (JCPDS Data No. 01-077-0244). Also intersection of lattice fringes are observed which is an indication of the overlap of several PbS nanoparticles with different orientations. Selected area electron diffraction (SAED) image shown in Fig. 8(c) exhibits multiple diffractions rings with missing periodicity which is due to the random orientation of the polycrystalline particles. No significant difference is observed in both the images except the difference in grain sizes. In both cases nearly spherical PbS nanoparticles are observed. They also reveal that small grains attach together and produce larger grains. TEM images of 1wt.% Mn doped PbS and 2 wt.% Mn doped PbS thin film as-prepared at concentration 0.2 M keeping constant pH value 11 and deposition temperature 313K are shown in Fig. 9(a-c) and Fig. 10(a-c) respectively. They also reveals that small grains attach together and produce large grains. The grains in dark colour shown in Fig. 9(a) and Fig. 10(a) are that of Mn doped PbS and the calculated average grain sizes are found to be in the ranges 11-14nm and 9-11 nm respectively which are almost in the range of the X-ray diffraction results 11 nm and 9 nm respectively. HRTEM is used to study the structure as well as to observe lattice images showing different orientations of the nanocrystals of Mn doped PbS. The HRTEM image shown in Fig. 8(b) depicts lattice fringes with d-spacing of 0.30 nm corresponding to (200) planes which is in good agreement with the lattice constant for the PbS cubic structure (JCPDS Data No. 01-077-0244) and Fig. 9 (b) exhibits lattice fringes with d-spacing of 0.25 nm to (200) plane of the Mn doped PbS cubic structure respectively. Also intersection of lattice fringes are observed which is an

indication of the overlap of several Mn doped PbS nanoparticles with different orientations. Selected area electron diffraction (SAED) image shown in Fig. 8(c) and Fig. 9(c) exhibit multiple diffraction rings with missing periodicity which is due to the random orientation of the polycrystalline particles. No significant difference is observed in both the images except the difference in grain sizes. In both cases nearly spherical Mn doped PbS nanoparticles are observed. From the TEM studies of undoped and doped PbS films, we observed that the d-value are slightly increased for the Mn-doped PbS films.

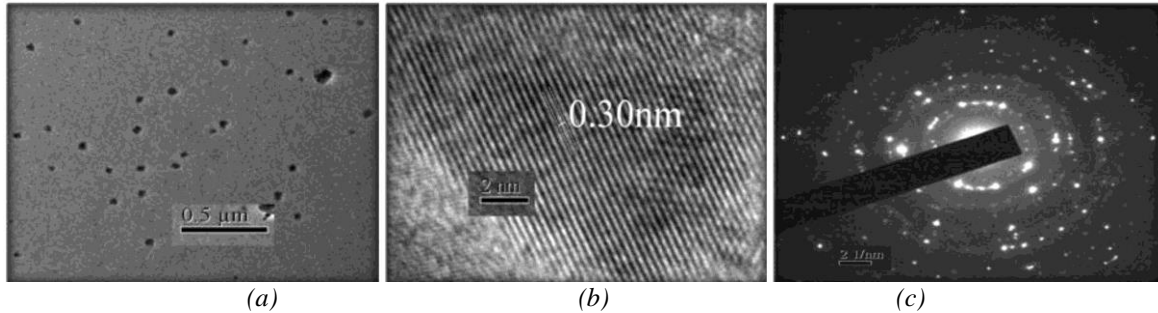


Fig.8.(a-c). (a) TEM image, (b) HRTEM image and interplanar spacing 'd' (c) SAED image of 0 wt. % Mn doped PbS.

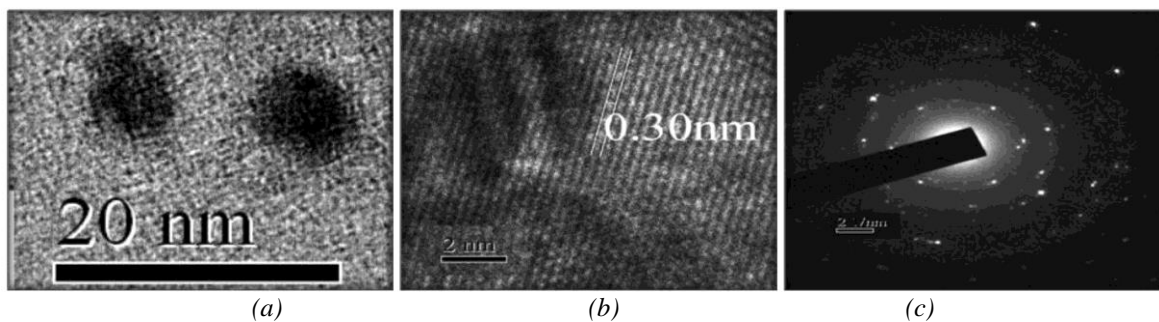


Fig. 9.(a-c). (a) TEM image, (b) HRTEM image and interplanar spacing 'd' (c) SAED image of 1 wt.% Mn doped PbS thin film.

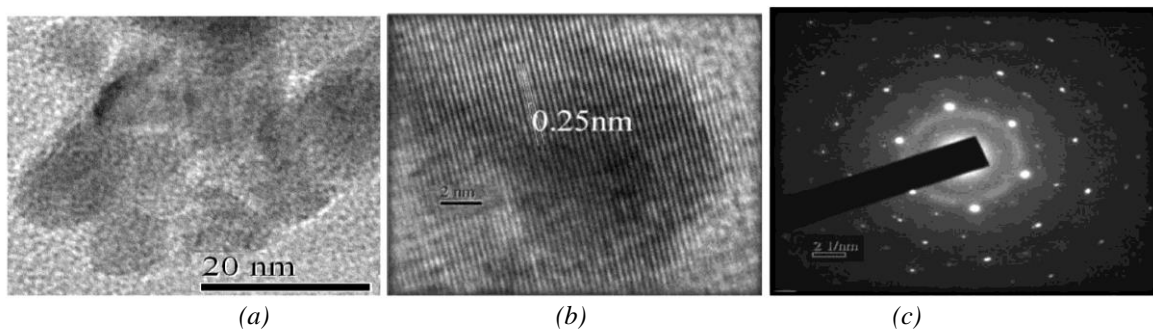


Fig.10. (a-c): (a) TEM image, (b) HRTEM image and interplanar spacing 'd' (c) SAED image of 2 wt.% Mn doped PbS.

4. Conclusions

Nanocrystalline undoped and Mn-doped PbS thin films were synthesized and deposited on glass substrates by CBD method. The overall surface morphology of the films from the SEM analysis shows that all the films are fairly smooth and uniform. The films consist of particles of different shape and sizes. The particle size determined from XRD and TEM are closely agreed.

Acknowledgments

One of the authors, L. Rajen Singh express our gratefulness to the Department of Instrumentation&USIC, SAIF, Gauhati University, Guwahati and Physics Department, Manipur University, Manipur for providing us the XRD and SAIF, NEHU, Shillong for TEM and SEM facilities. We acknowledge the Education Officer, UGC, NERO, Guwahati, for the fund provided vide UGC Financial Assistance Ref.No. F.5-177/2011-12/MRP/NERO/10721Dated 30 November 2011 (XI plan).

References

- [1] A. U. Ubale, A. R. Junghare, N. A. Wadbhasme, A. S. Daryapurkar, R.B. Mankar, V.S. Sangawar, *Turk.J. Phys.* **31**,279(2007).
- [2] L. Rajen Singh, S. Bobby Singh, A. Rahman, *Chalco. Let.***10**(5), 167 (2013).
- [3] Liu Xiaofei, ZhangMingde, *Int. J.Infrar.Millim. Wave***21**,1697 (2000).
- [4] K. M Gadave, S. A Jodgudri, C. D Lokhande, *Thin Solid Films***245**,7(1994).
- [5] J. Puiso, S. Tamulevicius, G. Laukaitis, S. Lindross, M. Leskeia, V. Snitka, *Thin Solid Films***403**,457(2002).
- [6] N. B. Kotadiya, A. J. Kothari, D. Tiwari, T. K. Chaudhuri, *Appl. Phys.A* **108**,819(2012).
- [7] P. Gadenne, Y. Yagil, G. Deutcher, *Journal of Applied Physics* **66**, (1989).
- [8] P.K. Nair, V.M. Garcia, A.B. Hernandez, M.T.S. Nair, *Journal of Physics D: Applied Physics* **24**, 1466 (1991).
- [9] I. Pop, C. Nascu, V. Ionescu, E. Indrea, I. Bratu, *Thin Solid Films* **307**, 240 (1997).
- [10] B. Thangaraju, P. Kaliannan, *Semiconductor Science and Technology***15**, 849 (2000).
- [11] P. Raji, C. Sanjeeviraja, K. Ramchandran, *Bull. Mater.Sc.* **28**(3), 233 (2005).
- [12] R. Sahraei, R.Shahriyar, S.Majles, M. H. Ara, A. Daneshfar, N. Shokri, *Prog. Colour colourants Coat.***3**,82 (2010).
- [13] Gary Hodes, *Chemical Solution Deposition of Semiconductor Films*, Marcel Dekker, Inc. 2002.
- [14] S. Mageswari, L. Dhivya, B. Planivel, R.Murugan, *Journal of Alloys and Compounds* **545**, 41 (2012).
- [15] R. K. Joshi, A. Kanjilal, H. K. Sehgal, *Nanotechnology***14**, 809 (2004).
- [16] N. F. Mott, E. A. Davis, *Electronics Processes in Non-Crystalline Materials*, Clarendon, Oxford, p. 428, 1979.
- [17] V. I. Levchenko, L. I. Postnova, V. P. Bondarenko, N. N. Vorozov, V. A. Yakovtseva, L. N. Dolgyi, *Thin solid films***348**, 141 (1999).
- [18] S. Seghaier, N. Kamoun, R. Brini, A. B. Amara, *Mater. Chem. Physics.* **97**,71 (2006).
- [19] J. J. V. Jauregu, R. R. Bon, A. M. Galvan, M. S. Lerma, *Thin Solid Films***441**, 104(2003).
- [20] E. Pentia, L. Pintillie, C. Tivarus, I. Pintillie, T. Botila, *Mater. Sci. Eng.* **B80**, 23(2001).
- [21] R. K. Joshi, A. Kanjilal, H. K. Sehgal, *Appl. Surf. Sci.* **221**,43(2004).
- [22] K. M. Gadave, S. A. Jodgudri, C. D. Lokhande, *Thin Solid Films* **245**,7(1994).
- [23] S. Bhushan, M. Mukharjee, P. Bose, *J. Mater. Sci. Mater. Electron.***13**, 581(2002).
- [24] Powder Diffract. File, JCPDS Internat. Centre Diffract. Data, PA 19073-3273, U.S.A.(2001)
- [25] H.K. Yadav, K. Sreenivas, R.S. Katiyar, V. Gupta, *J. Phys.* **40**, 6005 (2007).
- [26] N. Badera, B. Godbole, S.B. Srivastava, P.N. Vishwakarma, L.S.S. Chandra, D. Jain, M. Gangrade, T. Shripathi, V.G. Sathe, V. Ganesan, *Appl. Surf. Sci.* **254**, 7042 (2008).
- [27] B.D.Cullity, *Elements of X-ray Diffractation* (Massachusetts : Addison - Wesley. 102(1956)).
- [28] C.T. Tsai, S.H. Chen, D.S. Chuu, *Phys. Rev. B* **54**, 11555 (1996).
- [29] D.H. Kim, D.J. Lee, N.M. Kim, S.J. Lee, T.W. Kang, Y.D. Woo, D.J. Fu, *J. Appl. Phys.***101**,094111 (2007).
- [30] Juan Chu, Zhengguo Jin, Shu Cai, Jingxia Yang, Zhanglian Hong, *Thin Solid Films***520**, 182(2012).
- [31] R. Sahraei, S. Shahriyar, M. H. Majles Ara, A. Daneshfar, N. Shokri, *Prog. Color Colorants Coat.***3**,82 (2010).

- [32] S. Prabakar, M. Dhanam, Journal Crystal Growth **285**, 41 (2005).
- [33] S. Mageswari, L. Dhivya, B. Palanivel, R. Murugan, Journal of Alloys and Compounds **545**, 41 (2012).
- [34] B. Baruah, L. Saikia, M. N. Borah, K.C. Sarma, IOSR-JAP **5**(2),7(2013).